Supplementary Information For

Redox Programmable Delivery Systems: Sweet Block Copolymers Micelles via Thiol-(Bromo)Maleimide Conjugation

A. Petrelli, R. Borsali, S. Fort and S. Halila*

CERMAV, CNRS and Grenoble Alpes Université, 38000 Grenoble (France).

E-mail: sami.halila@cermav.cnrs.fr; Fax: +33-476-547-203

Table of contents

1. Materials

Hydroxy-terminated γ-polycaprolactone (PCL-OH; M_w = 4100 g mol^{-1}; PDI 1.2) was purchased from Polymer Source (Dorval, QC, Canada), and used as received. Dimethylaminopyridine (DMAP), dicyclohexylcarbodiimide (DCC), beta-alanine, diisopropylethylamine (DiPEA), maleic anhydride, bromomaleic anhydride were purchased from Sigma-Aldrich. Maleimidopropionic acid and bromo-maleimidopropionic acid were prepared following a previously described procedure.[1] *N*,*N*-dimethylformamide (DMF) was distilled under vacuum and stored over activated molecular sieves 4Å. Dichloromethane (DCM) was washed with deionized water to remove the ethanol stabilizer, followed by drying over calcium hydride and distilled. Tamarind seed Xyloglucan from Saiguru Food Gum manufacturer (Bombay, India) was previously purified by dissolving in deionized water (2% w/v), boiled for 1h then insoluble materials were removed by filtration. XGOs consisting of 7, 8 or 9 sugar units were prepared by enzymatic depolymerization of purified xyloglucan,[2] and subsequently modified to afford thiol-containing XGOs as already reported in our previous paper.[3]

2. Equipment

NMR analyses were recorded at 25°C on a Bruker Advance DRX400 spectrometer. Chemical shifts (δ) are given in ppm. The solvent residual peaks of D_2O, DMF, and $CDCl_3$ were used as internal standards, at 4.75 ppm, 8.03 ppm and 7.27 ppm, respectively. Matrix-assisted laser desorption ionization time-of-flight (MALDI-TOF) measurements were performed on a Bruker Daltonics Autoflex apparatus using 2,5-dihydroxybenzoic acid (DHB) as a matrix. High resolution mass spectrometry was carried on a Waters Xevo™ G2-S QTOF (quadrupole hybrid with orthogonal acceleration time-of-flight) mass spectrometer apparatus. For end-functionalized PCL and OBCPs, gel permeation chromatography (GPC) measurements were performed at 60 °C using 1260 Infinity GPC system (Agilent Technologies) (100 µL manual injection system, 1260 Agilent quaternary pump, 1260-MDS refractive index detector) equipped with two Agilent PolyPore PL1113-6500 columns (linear, 7.5 × 300 mm; particle size, 5 µm; exclusion limit, 200 – 2 000 000) in DMF containing lithium chloride (0.005 M) at the flow rate of 1.0 mL min^{-1}. Dynamic light scattering experiments were carried out at room temperature using an ALV laser goniometer, which consists of a 22 mW HeNe linearly polarized laser operating at a wavelength of 632.8 nm and an ALV-5000/EPP multiple τ digital correlator with 125 ns initial sampling time. Transmission electron microscopy (TEM) experiments were carried out using a CM220 Philips microscope. Fluorescence experiments were carried on a Perkin Elmer LS-50B spectrometer with a pulsed high pressure xenon source.

---

[1] D. H. Rich, P. D. Gesellchen, D. Tong, A. Cheung, C. K. Buckner, *J. Med. Chem.* **1975**, *18*, 1004-1010.
[2] S. Halila, M. Manguian, S. Fort, S. Cottaz, T. Hamaide, E. Fleury, H. Driguez, *Macromol. Chem. Phys.* **2008**, *209*, 1282-1290.
[3] A. Petrelli, R. Borsali, S. Fort, S. Halila, *Carbohydr. Polym.* **2015**, *124*, 109-116.

3. General procedures

3.1. Synthesis of reducing-end thiol-functionalized xylooligosaccharides (XGO-SH)

N-(*β*-xylooligosyl)-2-acetamido-1-ethanethiol were prepared according to procedure described in our previous work.[3] NMR and MALDI-TOF characterization confirmed the structure and purity of the product (Figure S5-S7).

3.2. Synthesis of maleimide end-functionalized PCL (PCL-maleimide)

The syntheses of PCL-(bromo)maleimide were performed by a Steglich esterification between PCL_{4100}-OH and maleimidopropionic acid or bromo-maleimidopropionic acid . Mono-hydroxy terminated polycaprolactone (PCL-OH) (0.2 mmol) was dissolved in DCM (10 mL) followed by the addition of maleimidopropionic acid or bromomaleimidepropionic acid (2 mmol) and DMAP (0.1 mmol). The solution was cooled down to 0°C and then DCC (2 mmol) was added. The reaction mixture was stirred for 1 h at 0°C, allowed to warm up to room temperature and stirred for 16 h. The white precipitate was removed by filtration and washed twice with DCM. The filtrate was concentrated to a final volume of 10 mL and the polymer was precipitated with cold methanol. The solid was rinsed twice with cold methanol, and then dried to afford the corresponding PCL-maleimide (66% yield) or PCL_{4100}-bromomaleimide (70% yield) as a white solid.

PCL-maleimide: Yield: 66%; ^{1}H NMR (400 MHz, $CDCl_3$), *δ* (ppm) 1.26 (t, *J*=7.09 Hz, 3 H C*H3*-CH2-) 1.39 (quin, *J*=7.64 Hz, 58 H, -CH2-C*H2*- CH2-) 1.55 - 1.74 (m, 118 H, -C*H2*-CH2-C*H2*) 2.31 (t, *J*=7.58 Hz, 58 H,- C(O)-C*H2*-) 2.63 (t, *J*=7.09 Hz, 2 H,-C(O)-C*H2*-) 3.83 (t, *J*=7.21 Hz, 2 H, N-C*H2*-) 3.97 - 4.10 (m, 60 H) 6.71 (s, 2 H,-C*H*=C*H*-); MALDI-TOF MS$^+$: $[M+Na]^+$ for $C_{189}H_{311}NO_{64}$(n=30) Calculated m/*z*= 3644.11 ; found = 3645.58 Mw/Mn = 1.04

PCL-bromomaleimide: Yield: 70%; ^{1}H NMR (400 MHz, $CDCl_3$), *δ* (ppm) 1.26 (t, *J*=7.09 Hz, 3 H C*H3*-CH2-) 1.41 (quin, *J*=7.64 Hz, 57 H, -CH2-C*H2*- CH2-) 1.55 - 1.74 (m, 117 H, -C*H2*-CH2- C*H2*) 2.31 (t, *J*=7.58 Hz, 57 H,- C(O)-C*H2*-) 2.65 (t, *J*=7.09 Hz, 2 H,-C(O)-C*H2*-) 3.87 (t, *J*=7.21 Hz, 2 H, N-C*H2*-) 4.05 - 4.16 (m, 59 H) 6.89 (s, 1 H,-C*H*=C(Br)-); MALDI-TOF MS$^+$: $[M+Na]^+$ for $C_{189}H_{310}BrNO_{64}$ (n=50) Calculated m/z =3724.02 found =3723.881; Mw/Mn = 1.05.

3.3. Synthesis of hybrid PCL-*b*-XGO

PCL-(bromo)maleimide (0.02 mmol) and XGO-SH (0.024 mmol) were dissolved in 1 mL of DMF and stirred under argon for 24 h. The copolymer was precipitated by adding MeOH/H_2O (8:2, v/v) solvent mixture, filtrated and washed with the same solvent mixture. The solid was dried under vacuum to yield the corresponding OBCP as a white solid.

PCL-b-XGO*:* Yield: 88%; ^{1}H NMR (400 MHz, DMF) *δ* ppm 1.22 (t, *J*=7.1 Hz 3H, (PCL) -CH_2-C*H*$_3$) 1.39 (quin, *J*=7.09 Hz, 70 H,(PCL) -CH_2-C*H*$_2$-CH_2-) 1.59 - 1.68 (m, 133 H,(PCL) -C*H*$_2$-CH_2-C*H*$_2$-) 2.35 (t, *J*=7.34 Hz, 70 H,(PCL)- C(O)-C*H*$_2$-) 3.20-3-80 (m, 70H, Carbohydrate, -C*H*$_2$-O-, -C*H*$_2$-C(O)-, -CO-C*H*$_2$-C*H*(S)-CO-) 3.95- 4.15 (m, 70 H, (PCL), –C(O)-O-*CH*$_2$-) 4.20-5.60 (m, 23H, Carbohydrate, -C*H*$_2$-O-, -C*H*$_2$-C(O)-, -CO-C*H*$_2$-C*H*(S)-CO-). MALDI-TOF MS$^+$: For *PCL-b-XGO*$_7$, $[M+Na]^+$ $C_{232}H_{384}N_2NaO_{97}S$ (n=20) / Calculated m/z = 4807.49, found = 4809.20;

for *PCL-b-XGO$_8$,* $[M+Na]^+$ $C_{238}H_{394}N_2NaO_{102}S$ (n=20) / Calculated m/z = 4969.54, found = 4971.58; for *PCL-b-XGO$_9$,* $[M+Na]^+$ $C_{244}H_{404}N_2NaO_{107}S$ (n=20) / Calculated m/z = 5131.59, found = 5133.66. Mw/Mn = 1.02 calculated for the (DP9).

PCL(ene)-b-XGO: Yield: 83%; ^{1}H NMR (400 MHz, DMF) δ ppm 1.22 (t, *J*=7.1 Hz 3H, (PCL) -CH_2-C*H$_3$*) 1.39 (quin, *J*=7.09 Hz, 70 H,(PCL) -CH_2-C*H$_2$*-CH_2-) 1.59 - 1.68 (m, 133 H,(PCL) -C*H$_2$*-CH_2-C*H$_2$*-) 2.35 (t, *J*=7.34 Hz, 70 H,(PCL)- C(O)-C*H$_2$*) 3.20-3-80 (m, 70H, Carbohydrate, -C*H$_2$*-O-, -C*H$_2$*-C(O)-, -CO-C*H$_2$*-C*H*(S)-CO-) 3.95- 4.15 (m, 70 H, (PCL), –C(O)-O-*CH$_2$*-) 4.20-5.60 (m, 23H, Carbohydrate, -C*H$_2$*-O-, -C*H$_2$*-C(O)-, -CO-C*H$_2$*-C*H*(S)-CO-) 7.07 (s, 1H, -C*H*=C(S)-). MALDI-TOF MS$^+$: For *PCL(ene)-b-XGO$_7$,* $[M+Na]^+$ $C_{232}H_{382}N_2NaO_{97}S$ (n=20) / Calculated m/z = 4805.47, found = 4807.46; for *PCL(ene)-b-XGO$_8$,* $[M+Na]^+$ $C_{238}H_{392}N_2NaO_{102}S$ (n=20) / Calculated m/z = 4967.52, found = 4969.10; for *PCL(ene)-b-XGO$_7$,* $[M+Na]^+$ $C_{244}H_{402}N_2NaO_{107}S$ (n=20) / Calculated m/z = 5130.58, found = 5131.31. Mw/Mn = 1.01 calculated for the (DP9)

3.4. Self-assembly of hybrid OBCPs by the co-solvent method (nanoprecipitation).

5 mg of the hybrid OBCP was dissolved in 2 mL of THF and stirred for 2 h then 10 mL of phosphate buffer (10 mmol, pH 7.4) was added at 0.1 mL min^{-1}. The solution was then stirred for one hour at 500 rpm and the organic solvent was removed by evaporation under reduced pressure until the final volume reached 5 mL. The solution of nanoparticles was then filtered through 0.45 µm Nylon membrane filter.

3.5. Encapsulation of Nile red by the co-solvent method

Nile red encapsulation was carried out with the co-solvent method as described above but the initial THF solution was replaced by a Nile red solution in THF at 0.0125 wt%.

3.6. Encapsulation efficiency

The encapsulation efficiency was evaluated by freeze-drying a determined withdrawn volume of nanoparticles suspension. The solid was then taken back in DMF, sonicated and the Nile red fluorescence of the sample was compared against a calibration curve. The encapsulation efficiency and loading were calculated according to the following equations:

$$Encapsulation\ efficiency = \frac{encapsulated\ Nile\ red}{total\ nile\ red\ amount} \times 100\%$$

$$Loading = \frac{Weight\ of\ loaded\ Nile\ red}{(weight\ of\ polymer)} \times 100\%$$

3.7. Dynamic light scattering measurements (DLS)

The nanoparticle suspensions were directly poured into the glass cells, and the measurements were carried out at a 90° angle with 60 s sampling time. In DLS, the relaxation time distribution was obtained using the CONTIN analysis of the autocorrelation function ($g^{(2)}-1$). From the linear dependence of the relaxation frequency ($1/\tau$) as a function of the squared wave vector modulus (q^2), the diffusion coefficient (D_{diff}) of the nanoparticles was calculated. The hydrodynamic radius (R_h) was then obtained from D_{diff} using the Stokes−Einstein relation.

3.8. Transmission electron microscopy (TEM) observations

TEM was carried out using a M200 Philips microscope (FEI Company, Hillsboro, OR, USA) operating at 80 kV, and images were recorded on Kodak SO163 films. A droplet of nanoparticle suspension was deposited onto glow-discharged carbon-coated copper grids and stained with uranium acetate. After a few minutes, the liquid in excess was blotted with filter paper and the sample was air-dried overnight prior to imaging.

4. Starting material characterization:

4.1. Xylogluco-oligosaccharides (XGO):

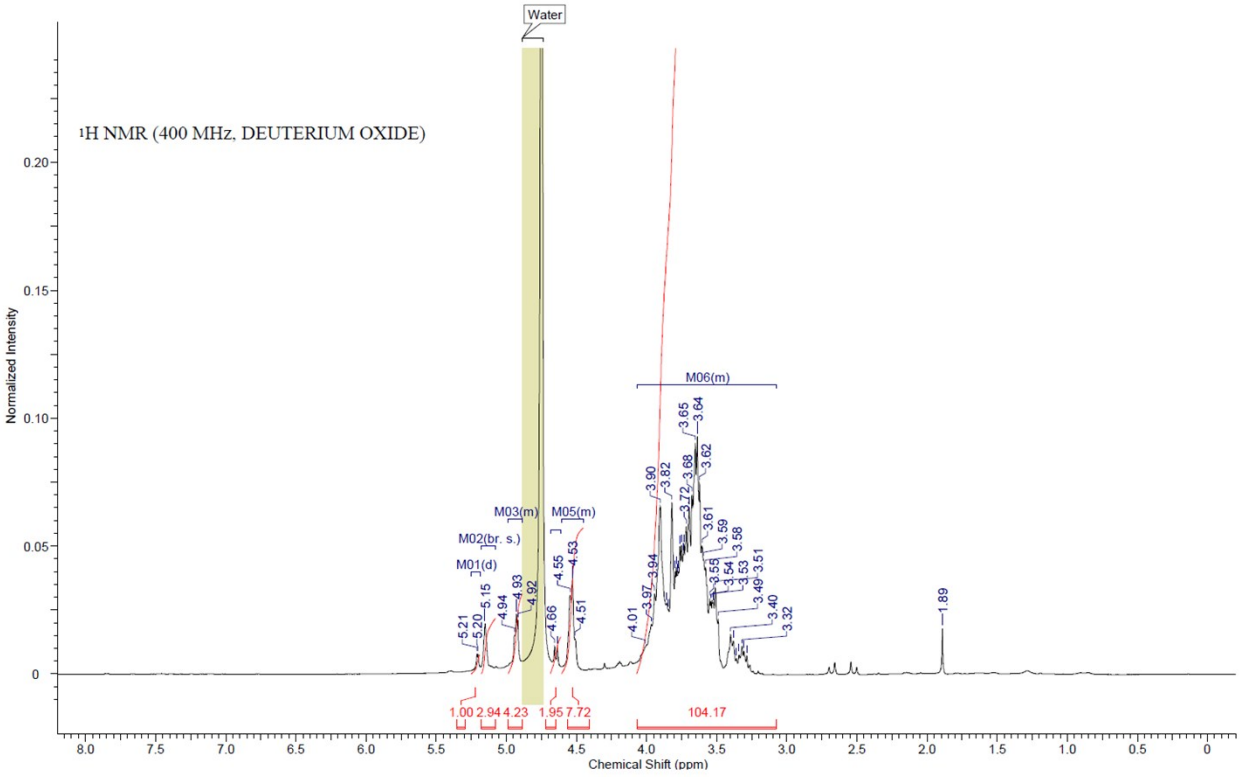

Fig. S1 ¹H NMR spectrum of XGOs (DP7, DP8 and DP9)

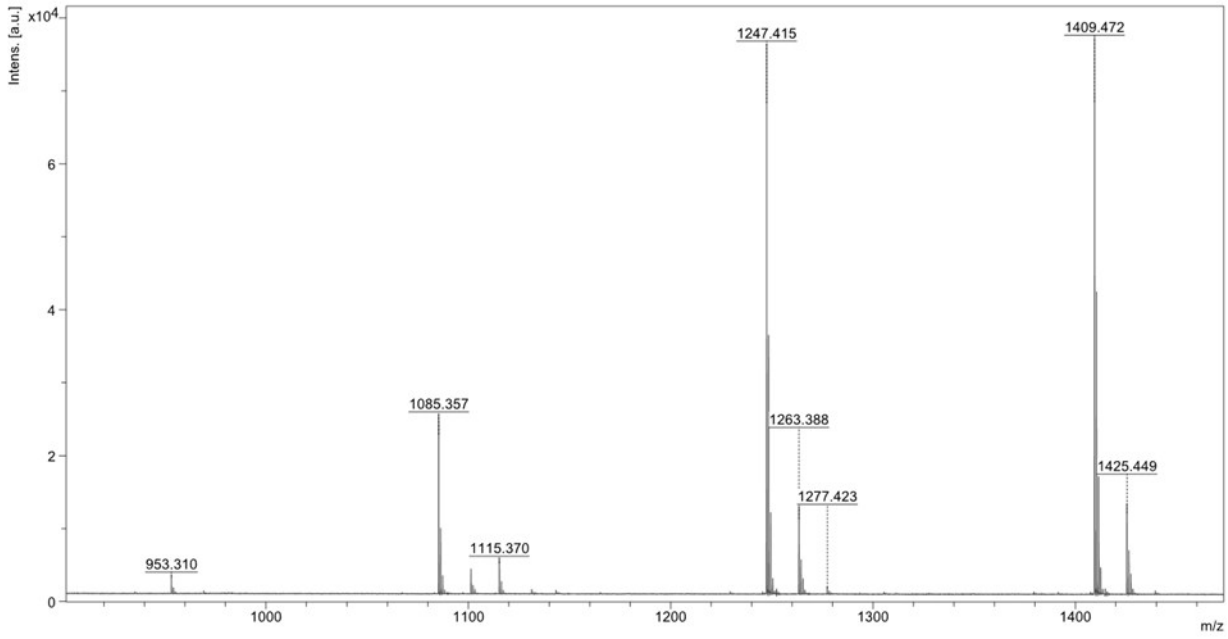

Fig. S2 MALDI-TOF mass spectrum of XGOs (DP7, DP8 and DP9)

4.2. PCL-OH :

^{1}H NMR (400 MHz, $CDCl_3$), δ (ppm) 1.26 (t, *J*=7.09 Hz, 3 H C*H3*-CH2-) 1.39 (quin, *J*=7.64 Hz, 58 H, -CH2-C*H2*- CH2-) 1.55 - 1.74 (m, 116 H, -C*H2*-CH2- C*H2*) 2.31 (t, *J*=7.58 Hz, 58 H,- C(O)-C*H2*-) 3.63 (t, *J*=7.21 Hz, 2 H, -C*H2*-OH) 3.97 - 4.10 (m, 54 H, -*CH2*-O-(CO)) 4.14 (q, *J*=7.09 Hz,2 H,-C*H2*-CH3)

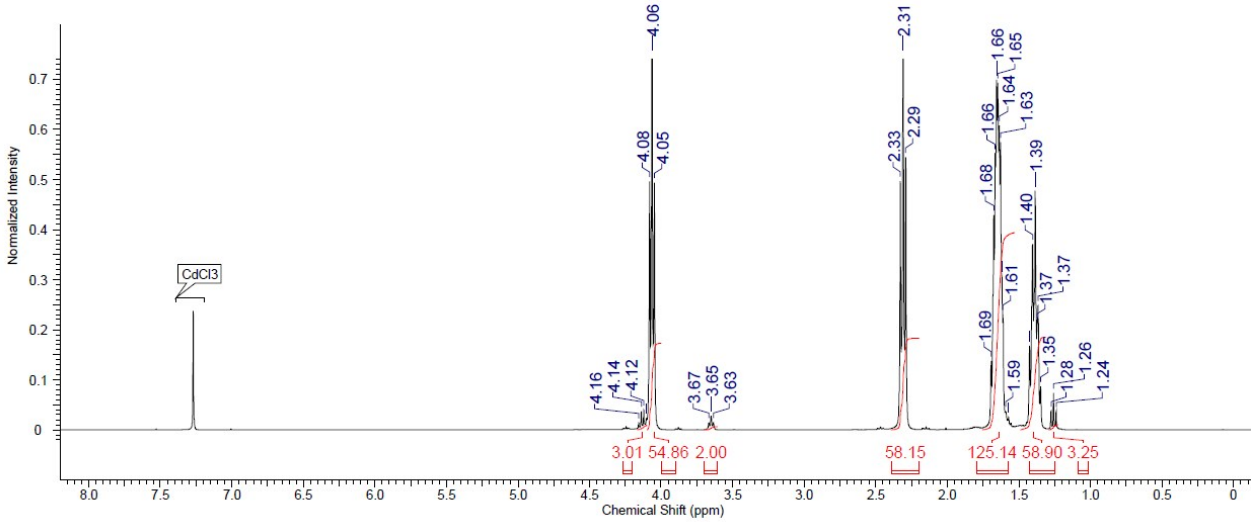

Fig. S3 ^{1}H NMR spectrum of PCL_{4100}-OH

MALDI-TOF MS^{+}: $[M+Na]^{+}$ for $C_{182}H_{306}NaO_{61}$ (n=30) Calculated m/z= 3493.08 ; found = 3493.96

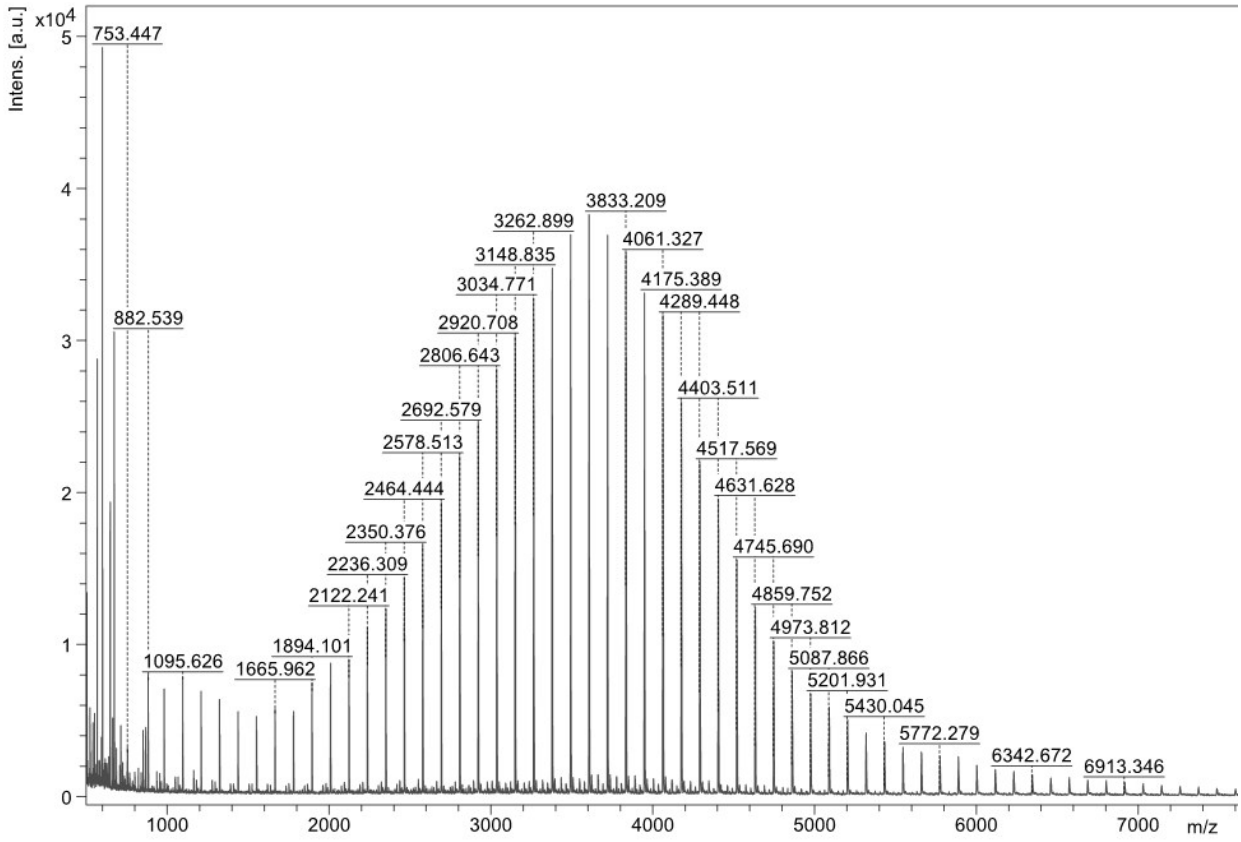

Fig. S4 MALDI-TOF mass spectrum of PCL-OH

4.3. *N*-(β-xyloglucooligosyl)-2-acetamino-1-ethanethiol (XGO-SH)

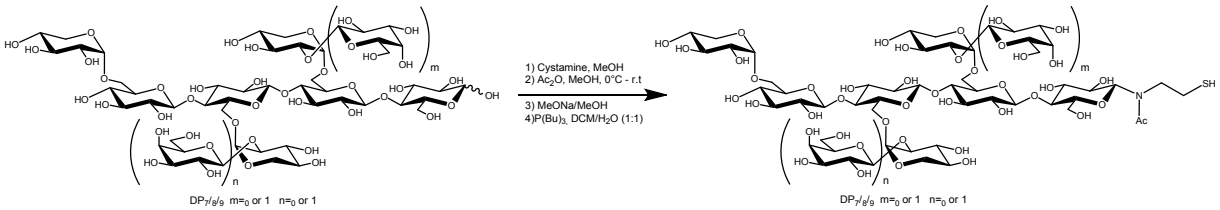

^{1}H NMR (400 MHz, D_2O), δ (ppm): 2.10-2.32 (2 x s, 3H, rotamers, -NCO*CH3*), 2.60 - 2.83 (m, 2H, C*H*2-SH), 3.29-4.02 (m, 51H, H-2,3,4,5,6 $^{GlcI–IV,Gal\ II-III}$, H-2,3,4,5$^{Xyl\ II-IV}$, NC*H*2), 4.45-4.62 (m, 4H, H-1$^{GlcII–IV,Gal\ II-III}$), 4.90 - 4.98 (m, 2H, H-1$^{XylIII-III}$), 5.02

(d, J = 8.3 Hz, 1H, H-1^{GlcI}, rotamer I), 5.17 (d, J = 2.4 Hz, 1H, H-1 ^{XylIV}), 5.40 (d, J = 8.6 Hz, H-1^{GlcI}, rotamer II);

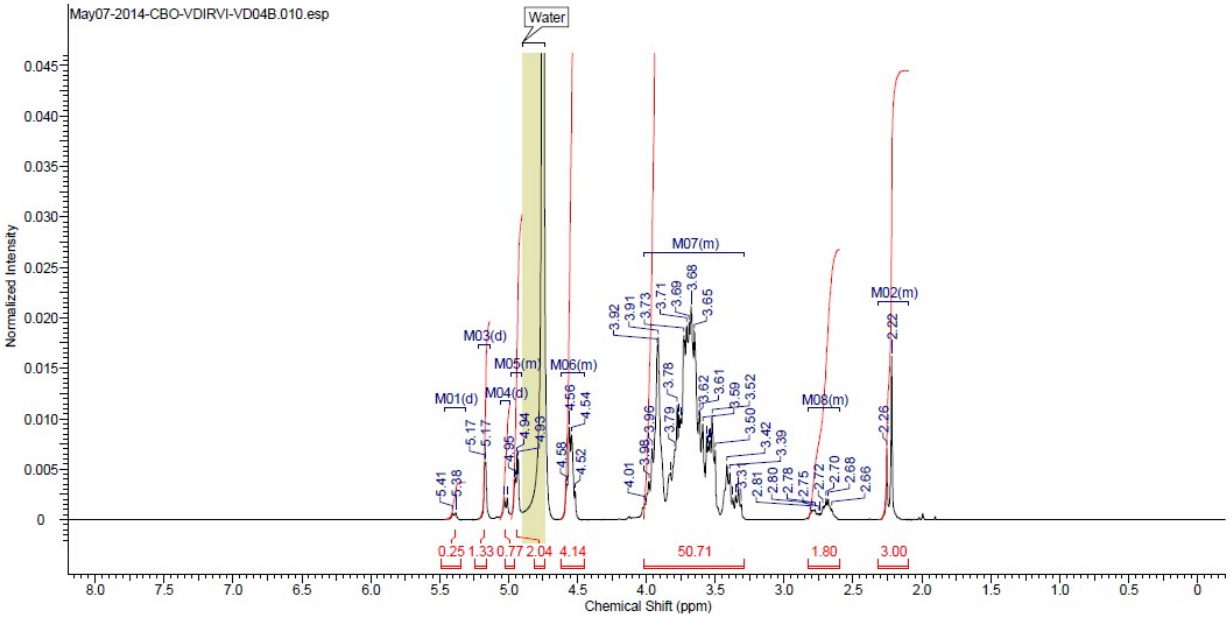

Fig. S5 ^{1}H NMR spectrum of XGOs-SH

^{13}C NMR (100MHz, D_2O), δ (ppm) 21.3, 21.7, 22.0, 23.3 (2 x 1C, rotamers, -*C*H2-SH), 60.1, 61.0, 61.2, 61.5, 65.9, 66.7, 68.6, 69.4, 69.5, 69.5, 69.9, 71.1, 71.5, 71.9, 72.6, 72.7, 73.0, 73.3, 73.6, 74.1, 74.3, 75.1, 75.6, 76.8, 78.7, 79.8, 80.2, 86.7, 98.3, 98.9, 102.6, 102.9, 103.0, 104.5, 175.5, 176,5 (2 x 1C, rotamers, -N*C*OCH3);

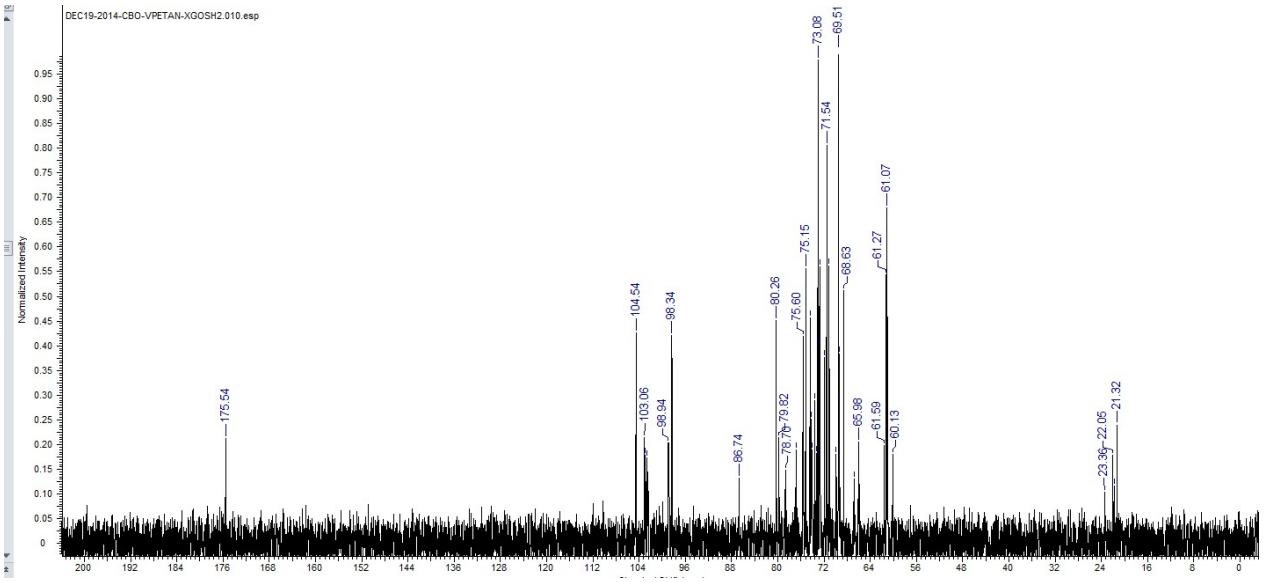

Fig. S6 ^{13}C NMR spectrum of XGOs-SH

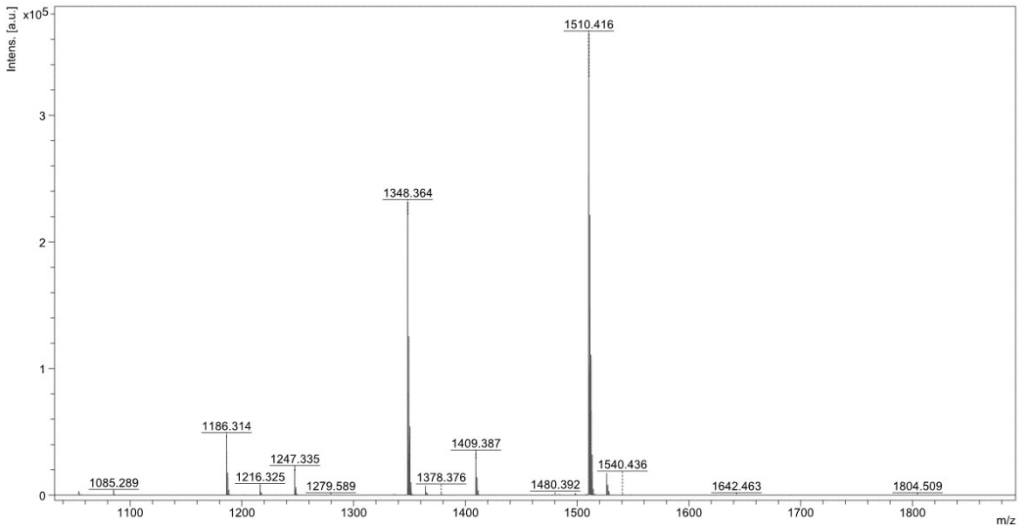

Fig. S7 MALDI-TOF mass spectrum of XGOs-SH

MALDI-TOF MS$^+$:**DP$_7$** $[M+Na]^+$ for $C_{43}H_{73}NO_{33}S$ calculated m/z = 1186.37 found m/z = 1186.31
MALDI-TOF MS$^+$:**DP$_8$** $[M+Na]^+$ for $C_{49}H_{83}NO_{38}S$ calculated m/z = 1348.42 found m/z = 1348.36
MALDI-TOF MS$^+$:**DP$_9$** $[M+Na]^+$ for $C_{55}H_{93}NO_{43}S$ calculated m/z = 1510.47 found m/z = 1510.42

4.4. PCL-maleimide

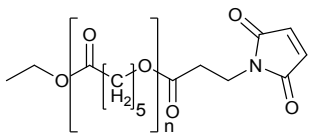

^{1}H NMR (400 MHz, $CDCl_3$), δ (ppm) 1.26 (t, *J*=7.09 Hz, 3 H C*H3*-CH2-) 1.39 (quin, *J*=7.64 Hz, 58 H, -CH2-C*H2*- CH2-) 1.55 - 1.74 (m, 118 H, -C*H2*-CH2- C*H2*) 2.31 (t, *J*=7.58 Hz, 58 H,- C(O)-C*H2*-) 2.63 (t, *J*=7.09 Hz, 2 H,-C(O)-C*H2*-) 3.83 (t, *J*=7.21 Hz, 2 H, N-C*H2*-) 3.97 - 4.10 (m, 60 H) 6.71 (s, 2 H,-C*H*=C*H*-)

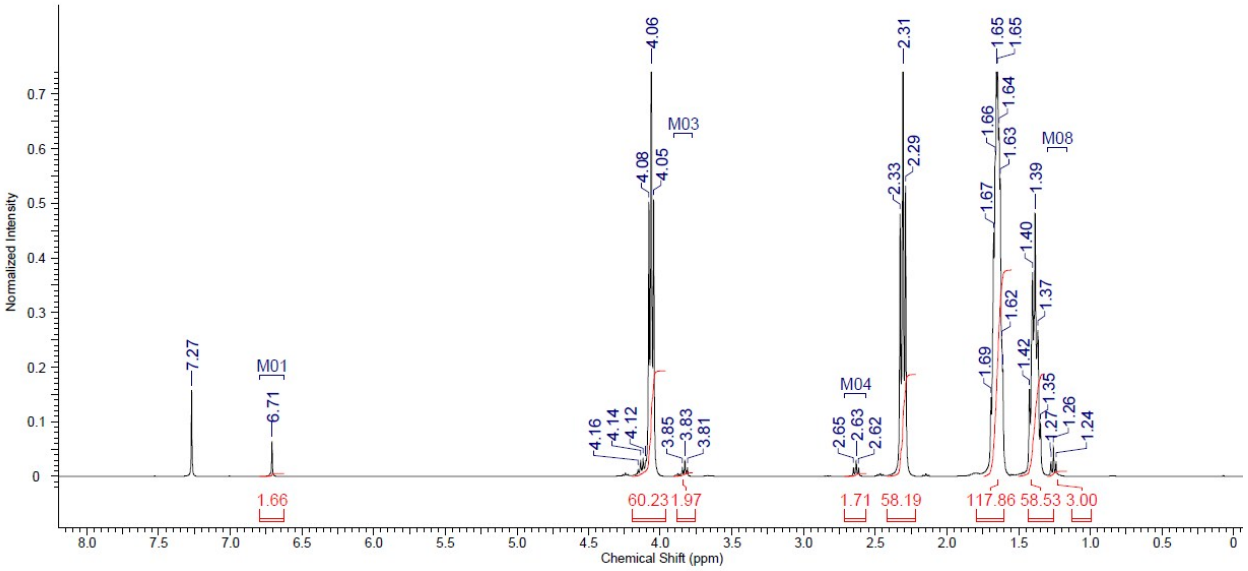

Fig. S8 ^{1}H NMR spectrum of PCL-maleimide

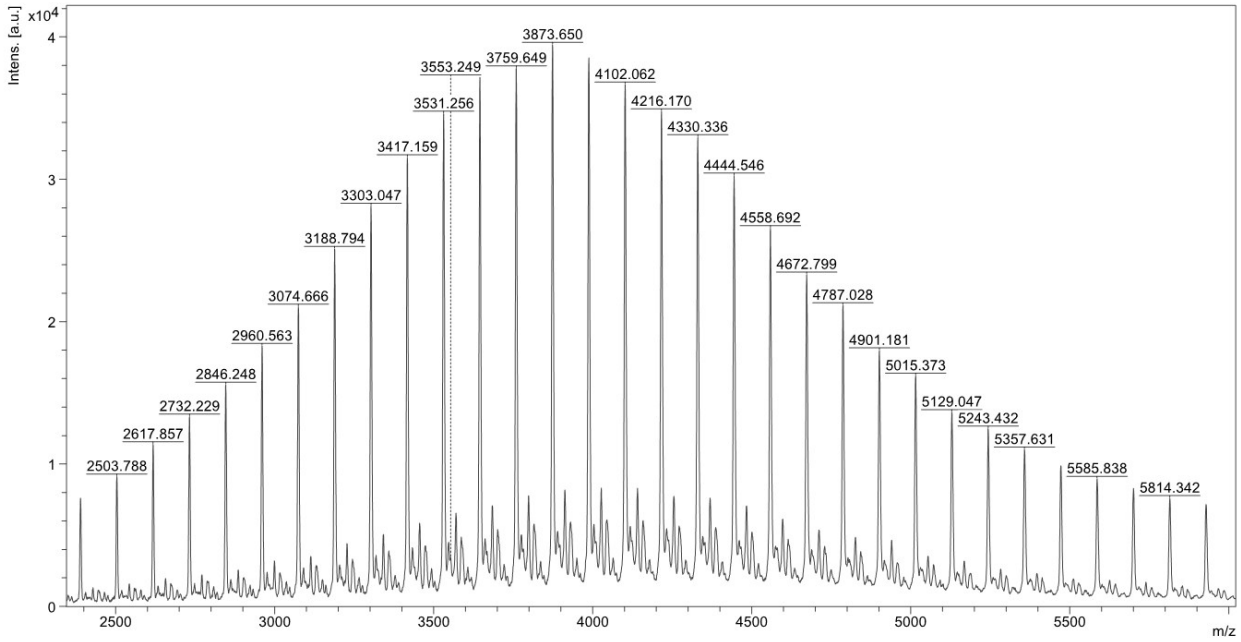

Fig. S9 MALDI-TOF mass spectrum of PCL-maleimide

MALDI-TOF MS$^+$: $[M+Na]^+$ for $C_{189}H_{311}NO_{64}$(n=50) Calculated m/z= 3644.11 ; found = 3645.58

4.5. PCL-bromomaleimide

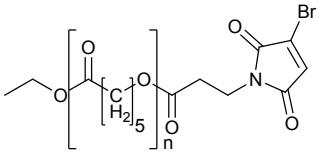

^{1}H NMR (400 MHz, $CDCl_3$), δ (ppm) 1.26 (t, *J*=7.09 Hz, 3 H C*H3*-CH2-) 1.41 (quin, *J*=7.64 Hz, 57 H, -CH2-C*H2*- CH2-) 1.55 - 1.74 (m, 117 H, -C*H2*-CH2- C*H2*) 2.31 (t, *J*=7.58 Hz, 57 H,- C(O)-C*H2*-) 2.65 (t, *J*=7.09 Hz, 2 H,-C(O)-C*H2*-) 3.87 (t, *J*=7.21 Hz, 2 H, N-C*H2*-) 4.05 - 4.16 (m, 59 H) 6.89 (s, 1 H,-C*H*=C(Br)-)

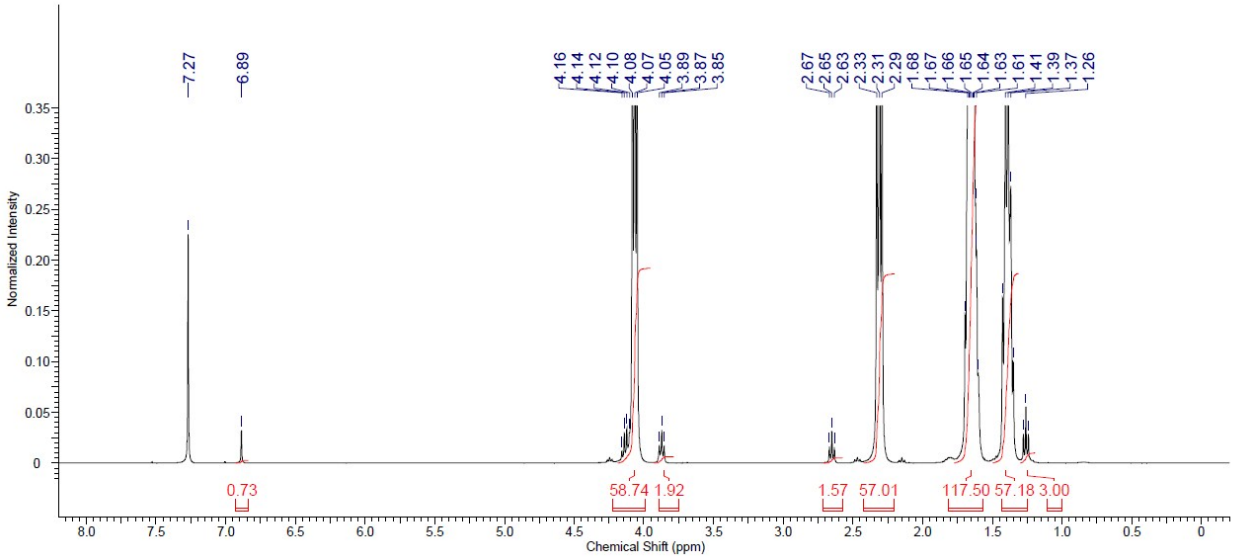

Fig. S10 ^{1}H NMR spectrum of PCL-bromomaleimide

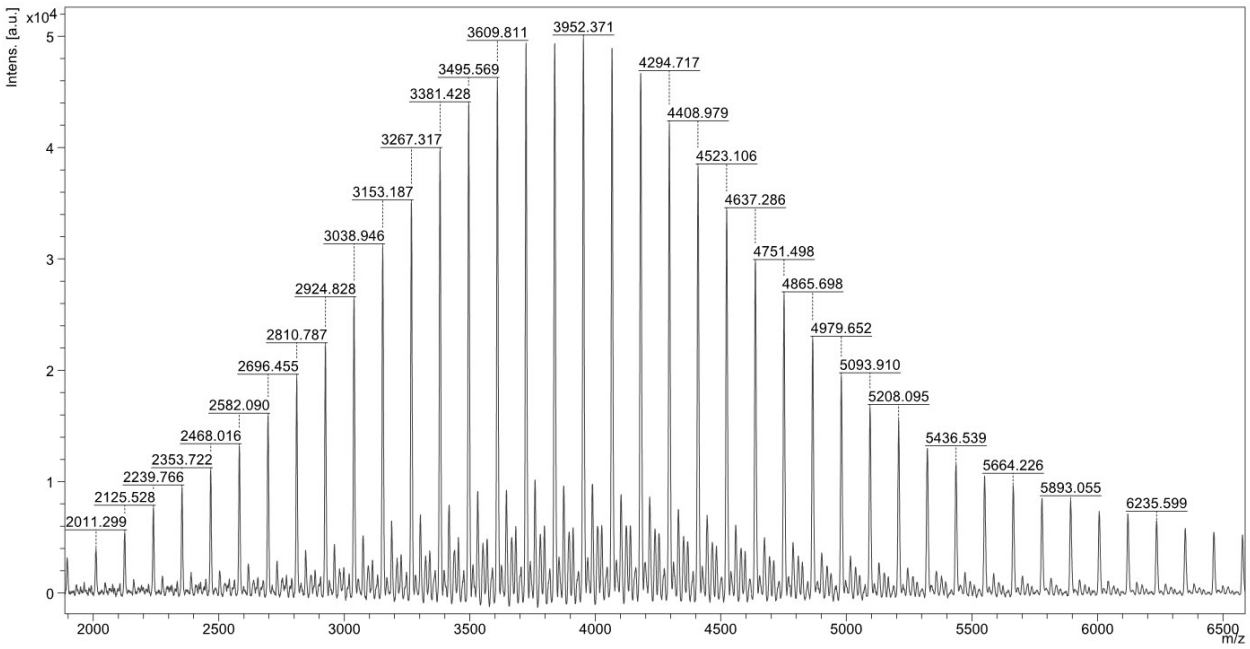

Fig. S11 MALDI-TOF mass spectrum of PCL-bromomaleimide

MALDI-TOF MS^+: $[M+Na]^+$ for $C_{189}H_{310}BrNO_{64}$ (n=50) Calculated m/z =3724.02 found =3723.881

4.6. PCL-*b*-XGO

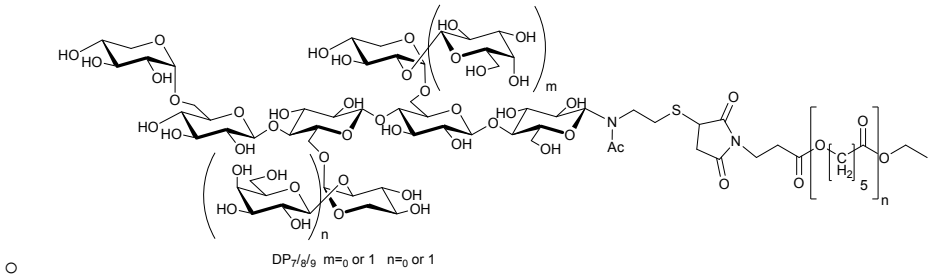

Yield: 88%; 1H NMR (400 MHz, DMF-d6) δ ppm 1.22 (t, J=7.1 Hz 3H, (PCL) -CH2-CH3) 1.39 (quin, J=7.09 Hz, 70 H,(PCL) -CH2-CH2-CH2-) 1.59 - 1.68 (m, 133 H,(PCL) -CH2-CH2-CH2) 2.35 (t, J=7.34 Hz, 70 H,(PCL)- C(O)-CH2) 3.20-3-80 (m, 70H, Carbohydrate, -CH2-O-, -CH2-C(O)-, -CO-CH2-CH(S)-CO-) 3.95- 4.15 (m, 70 H, (PCL), –C(O)-O-CH2-) 4.20-5.60 (m, 23H, Carbohydrate, -CH2-O-, -CH2-C(O)-, -CO-CH2-CH(S)-CO-).

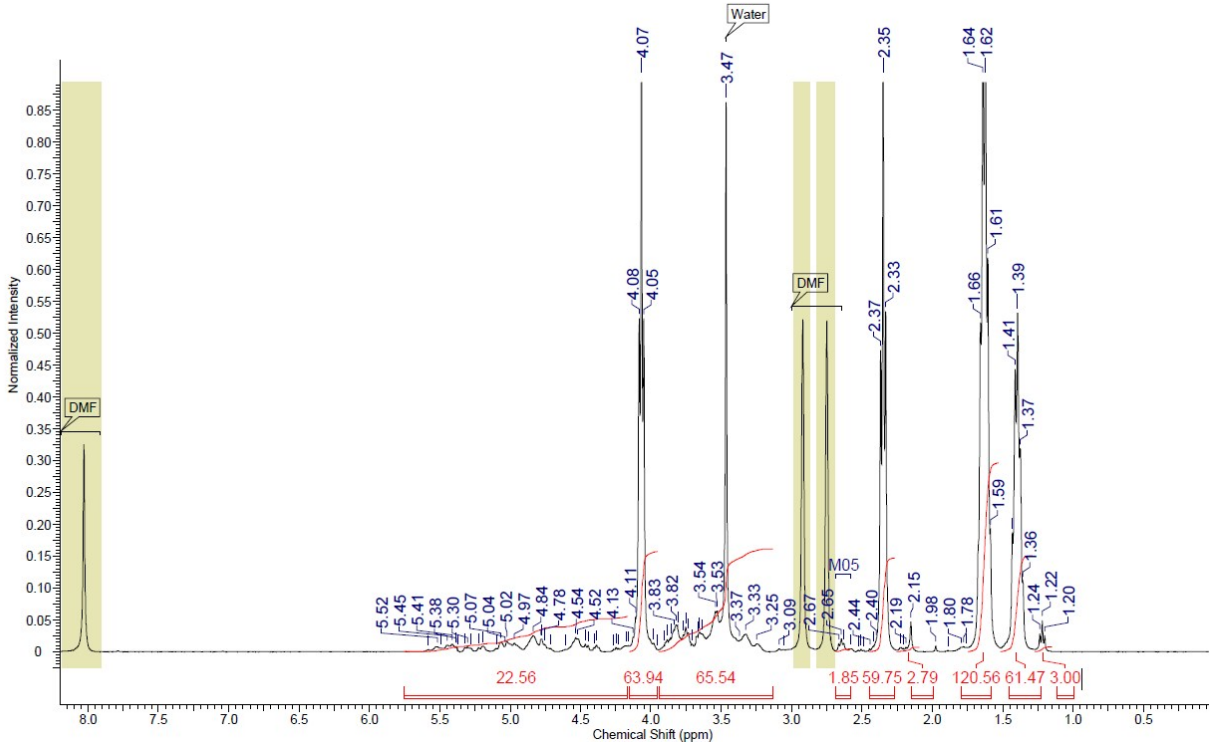

Fig. S12 ^{1}H NMR spectrum of PCL-*b*-XGO

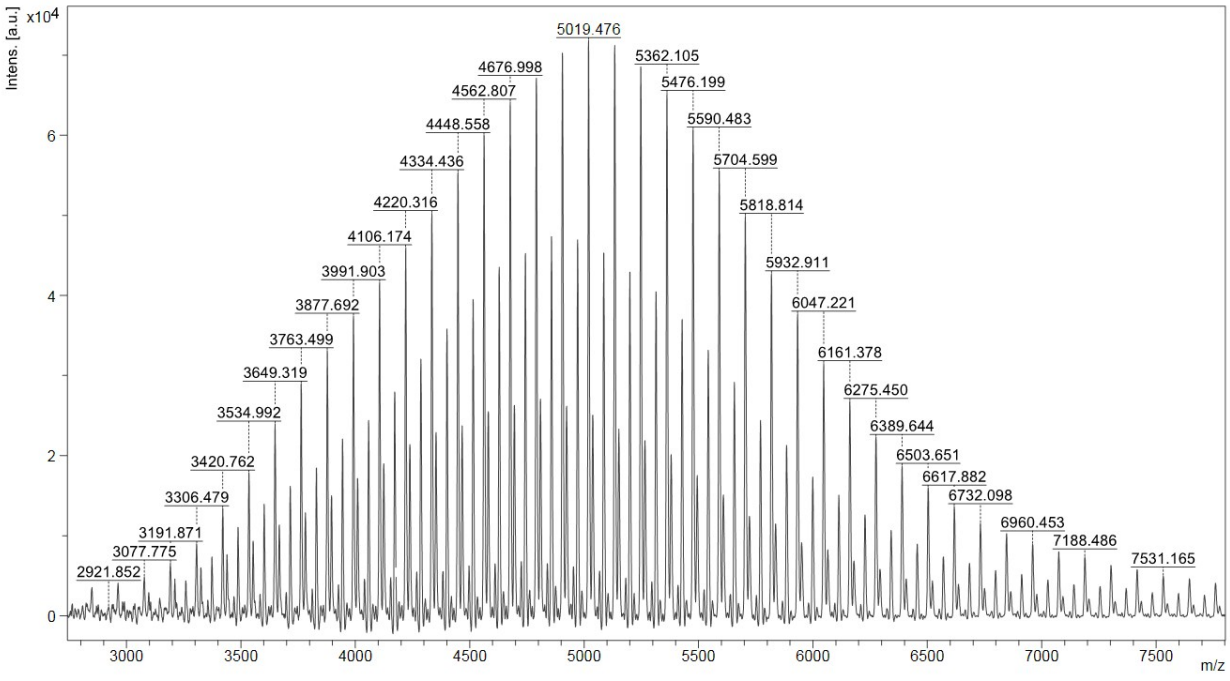

Fig. S13 MALDI-TOF mass spectrum of PCL-*b*-XGO

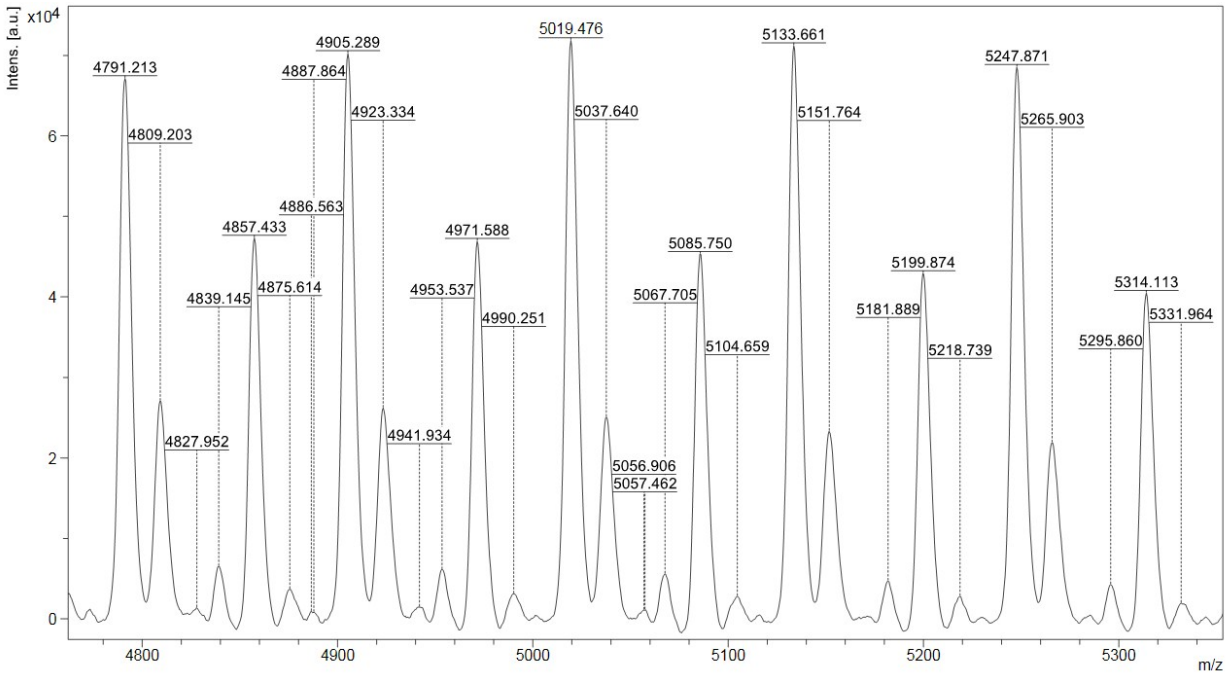

Fig. S14 Enlarged MALDI-TOF mass spectrum of PCL-*b*-XGO

MALDI-TOF MS^{+}: $[M+Na]^{+}$ $C_{232}H_{384}N_2NaO_{97}S$ (n=20) / **DP7** Calculated m/z = 4807.49 found = 4809.20

MALDI-TOF MS^{+}: $[M+Na]^{+}$ $C_{238}H_{394}N_2NaO_{102}S$ (n=20) / **DP8** Calculated m/z = 4969.54 found = 4971.58

MALDI-TOF MS^{+}: $[M+Na]^{+}$ $C_{244}H_{404}N_2NaO_{107}S$ (n=20) / **DP9** Calculated m/z = 5131.59 found = 5133.66

4.7. PCL(ene)-*b*-XGO:

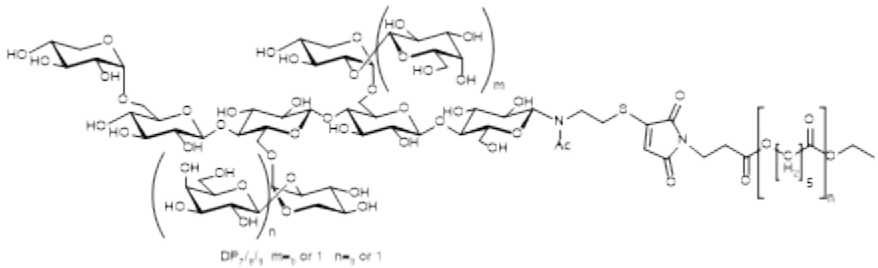

Yield: 83%; 1H NMR (400 MHz, DMF) δ ppm 1.22 (t, J=7.1 Hz 3H, (PCL) -CH2-CH3) 1.39 (quin, J=7.09 Hz, 70 H,(PCL) -CH2-CH2-CH2-) 1.59 - 1.68 (m, 133 H,(PCL) -CH2-CH2-CH2) 2.35 (t, J=7.34 Hz, 70 H,(PCL)- C(O)-CH2) 3.20-3-80 (m, 70H, Carbohydrate, -CH2-O-, -CH2-C(O)-, -CO-CH2-CH(S)-CO-) 3.95- 4.15 (m, 70 H, (PCL), –C(O)-O-CH2-) 4.20-5.60 (m, 23H, Carbohydrate, -CH2-O-, -CH2-C(O)-, -CO-CH2-CH(S)-CO-) 7.07 (s, 1H, -CH=C(S)-);

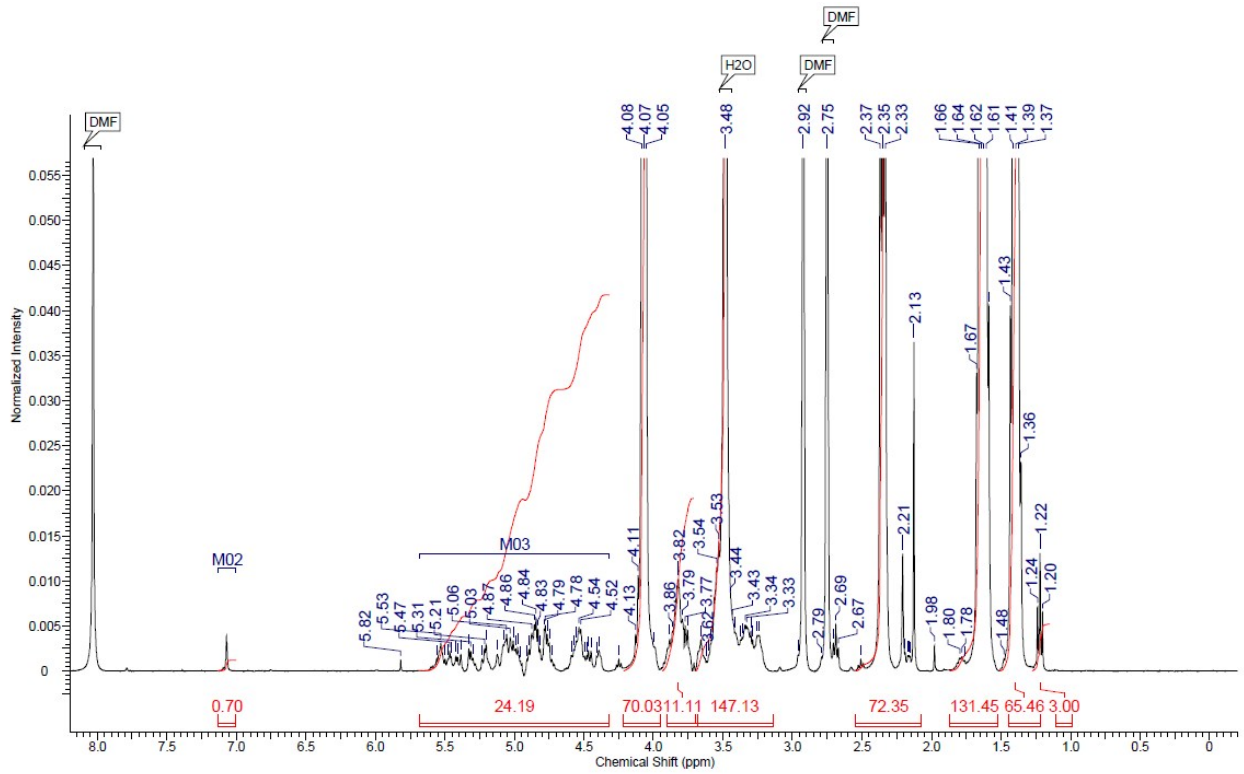

Fig. S15 ^{1}H NMR spectrum of PCL(ene)-*b*-XGO

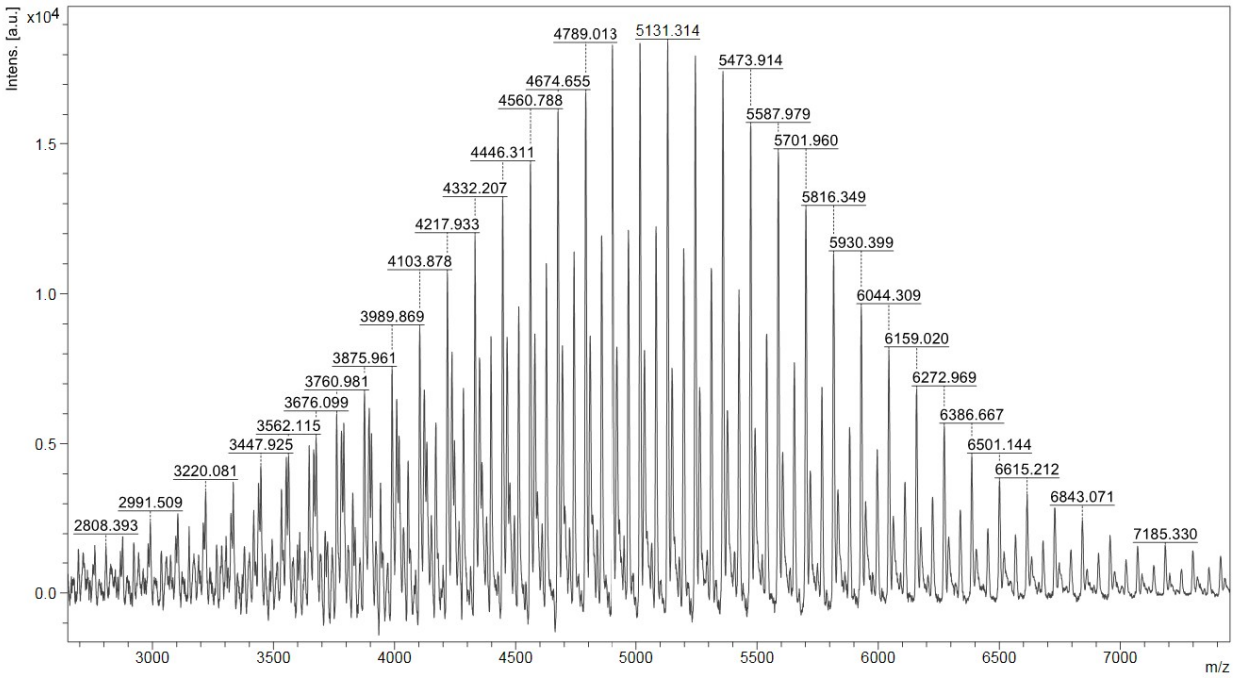

Fig. S16 MALDI-TOF mass spectrum of PCL(ene)-*b*-XGO

MALDI-TOF MS^{+}: $[M+Na]^{+}$ $C_{232}H_{382}N_2NaO_{97}S$ (n=20) / **DP7** Calculated m/z = 4805.47 found = 4807.46

MALDI-TOF MS^{+}: $[M+Na]^{+}$ $C_{238}H_{392}N_2NaO_{102}S$ (n=20) / **DP8** Calculated m/z = 4967.52 found = 4969.10

MALDI-TOF MS^{+}: $[M+Na]^{+}$ $C_{244}H_{402}N_2NaO_{107}S$ (n=20) / **DP9** Calculated m/z = 5130.58 found = 5131.31

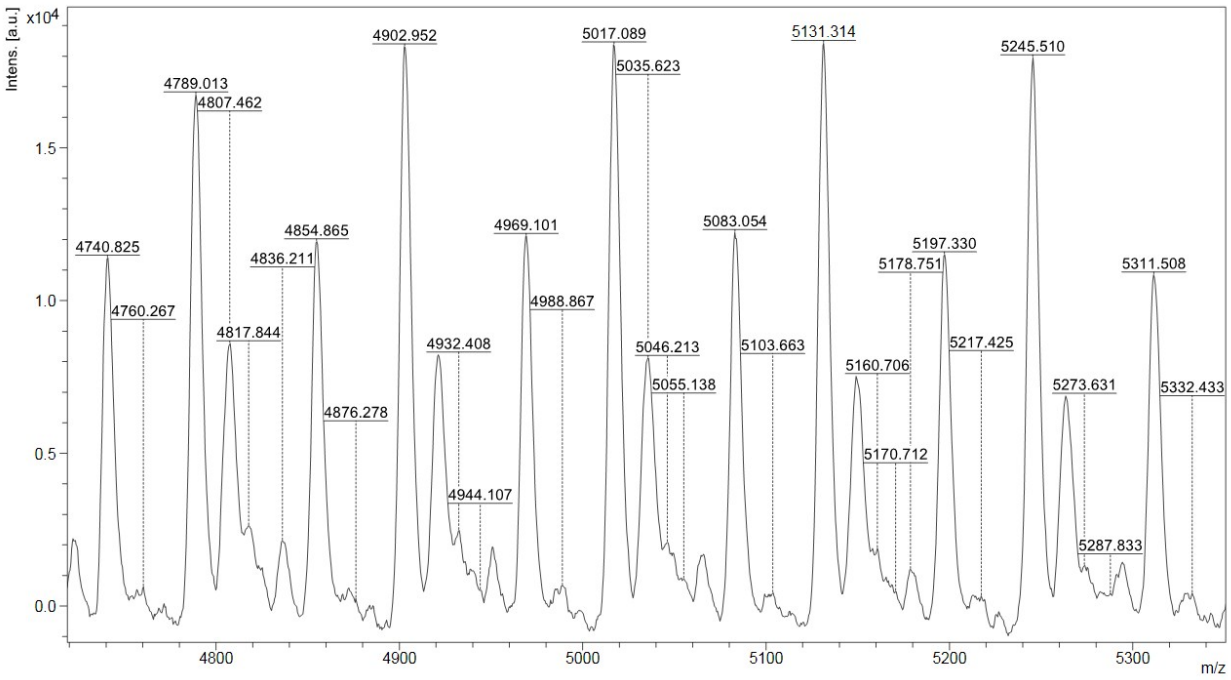

Fig. S17 Enlarged MALDI-TOF mass spectrum of PCL (ene)-*b*-XGO

5. GPC analysis in DMF(LiCl)

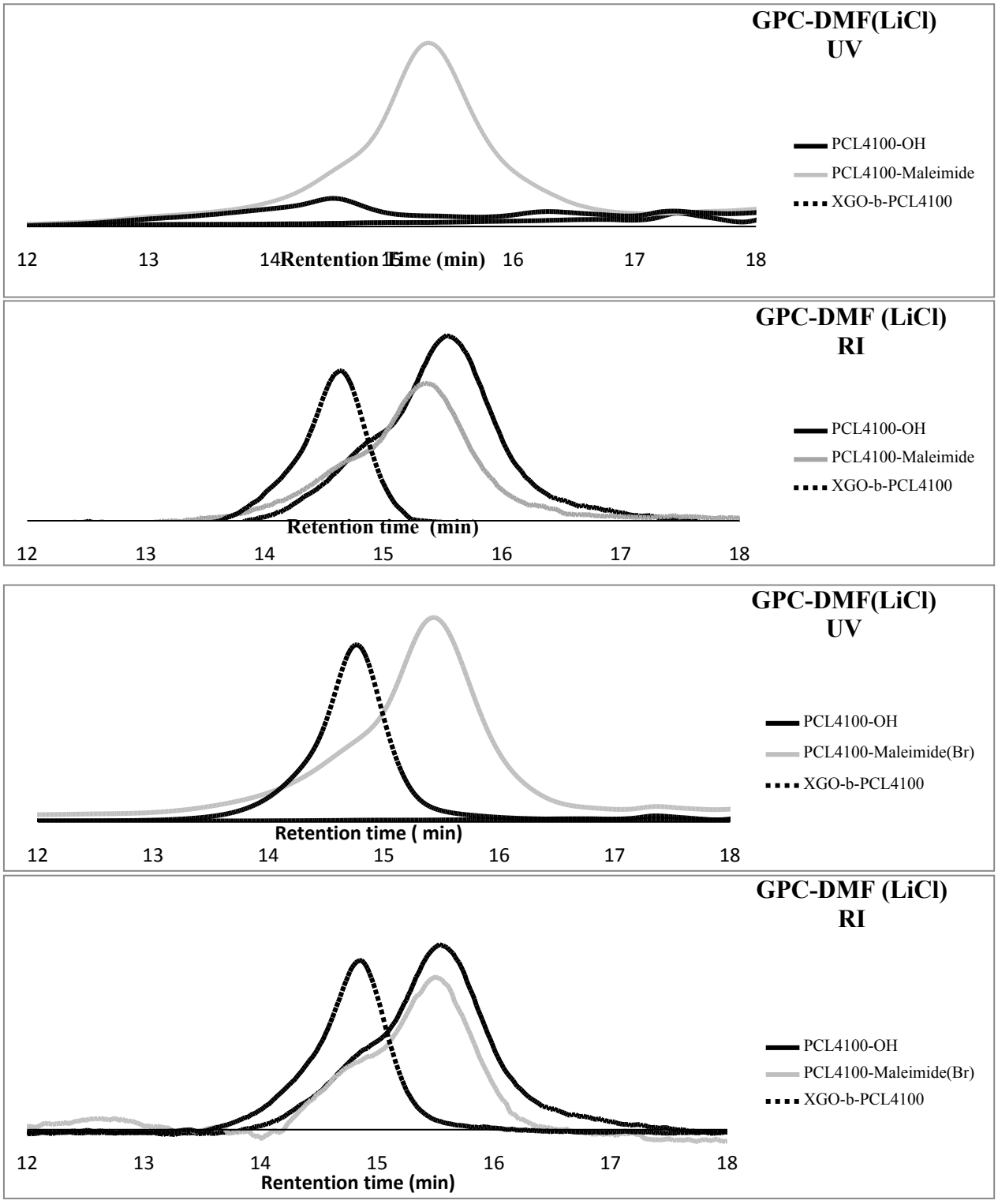

Fig. S18 GPC traces (DMF as eluent) of PCL-OH, PCL-maleimides, and PCL based block copolymers

6. Nanoparticles DLS analysis

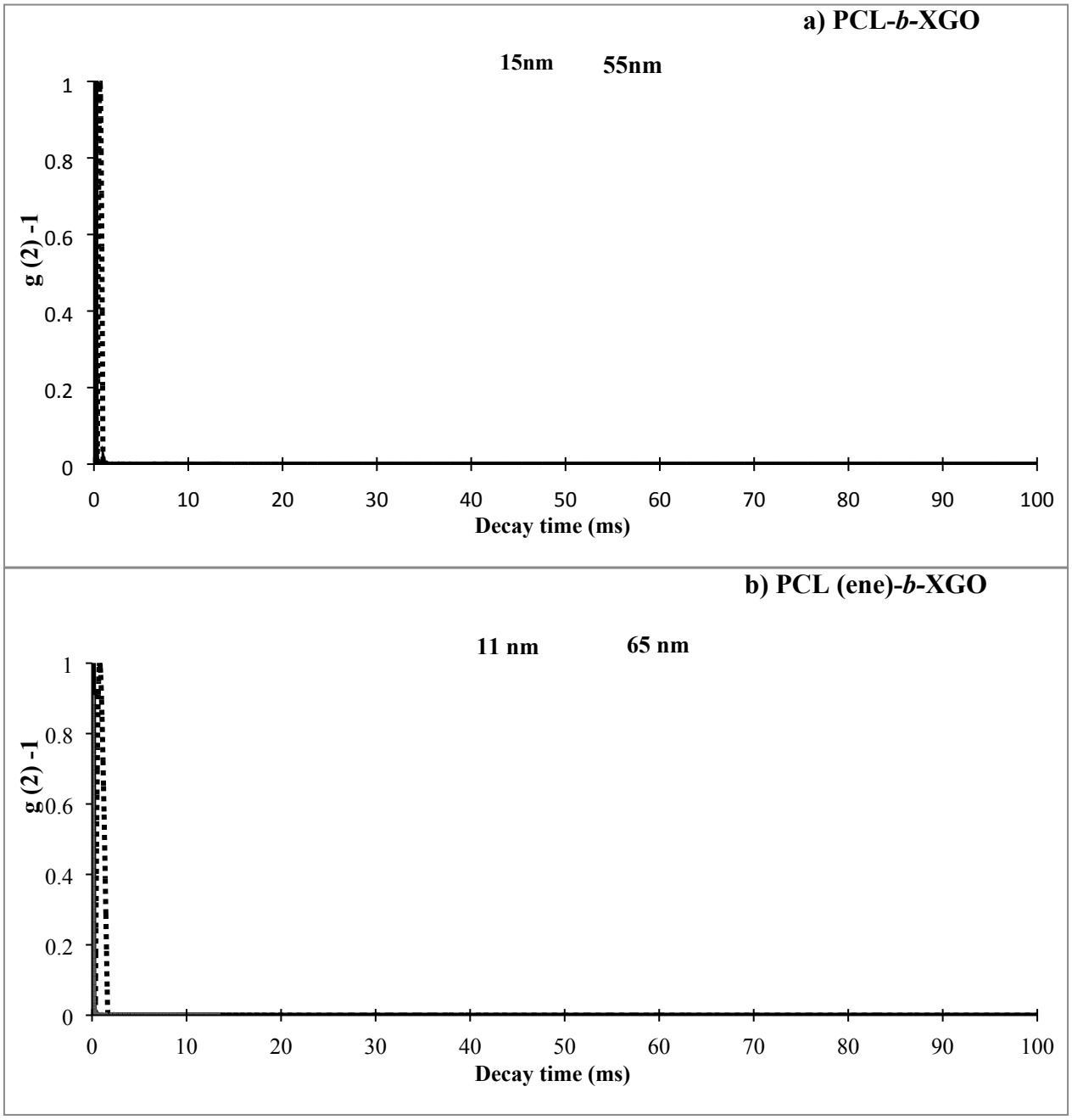

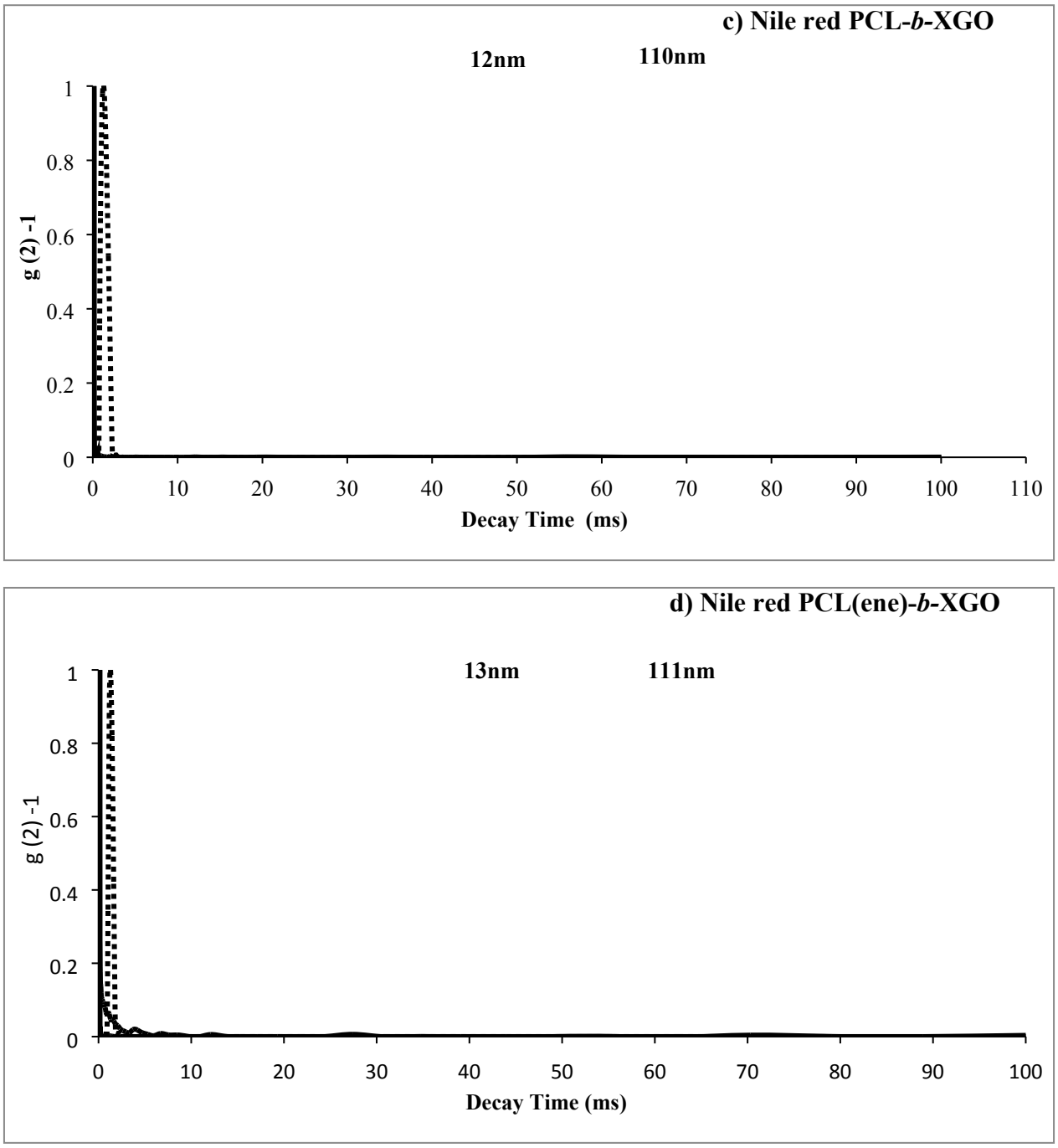

Fig. S19 DLS autocorrelation function ($g^{(2)}$-1) at 90°, weight (dashed line) and number (plain line) radius distribution of the xyloglucan oligosaccharide PCL in phosphate buffer at 25°C (c= 1mg.mL-1)